CHAPTER 8 – CONCLUSIONS AND RECOMMENDED WORK

8.1 Conclusions

The primary emphasis of this work is the application of modeling and automated classification in the development, validation, and implementation of non-destructive inspection techniques. These tools were used to develop ultrasonic inspection techniques for radial fatigue cracks located about four different cylindrical hole configurations: the empty cylindrical hole, the fluid-filled cylindrical hole, the cylindrical hole containing an elastic lining, and the cylindrical hole containing an elastic insert. Due to constraints on the placement of the transducer relative to the hole, special ultrasonic NDE techniques were explored for the detection and sizing of cracks at the bottom and top locations.

Typical C-scan pulse-echo ultrasonic inspection for bottom crack detection in weep holes was found to miss certain small cracks. To simulate the inspection problem, a 2D boundary element method (BEM) simulation was applied for the total field response generated by an ultrasonic transducer signal incident on a cylindrical hole with a surface breaking crack or notch. A technique was developed which examines the variation in the A-scan signals as the transducer is incrementally moved along the wing surface across the region of a weep hole. Studies of both experimental and simulated BEM signals were used to develop this approach. The performance of the automated spatial signal variation

(SSV) approach was found to exceed the performance of manual C-scan inspection. The advantage of this refined B-scan classification technique is the ability to detect superimposed signals independently from the general shape of the transient pulse.

Development, validation and implementation of a neural network assisted, automated ultrasonic inspection technique for the detection of bottom and top cracks on weep holes were completed. Toward achieving the goal of field implementation of an automated inspection technique, this work demonstrated the value of numerical simulation, laboratory studies and algorithm training with samples representing in-field variation, as well as in-field demonstration, parametric sensitivity studies, and probability of detection (PoD) validation. The inspection capability of the automated procedure was found to exceed both the defined inspection requirements and the ability of inspection through viewing C-scan images.

Ray analysis, analytical models and boundary element method (BEM) simulations were used to understand the nature of secondary reflected and transmitted signals from notches on an empty cylindrical hole. From these simulated results, a methodology for sizing top notches was proposed. A validation with experimental results was carried out.

A top crack inspection technique for fluid-filled weep holes was also investigated. A BEM model was applied for the scattering response of an incident shear wave transducer signal by a fluid-filled cavity with a fluid-filled notch. A viable ultrasonic inspection strategy was developed from the simulated studies. Validation of the approach was presented for both simulated and experimental data for top notches.

Models were used to investigate the effect of a polyurathane lining on the inside surface of the C-141 weep holes. The effect of an elastic layer on the propagation of 'leaky' Rayleigh waves about a cylindrical hole was investigated. First, the dispersion relations for this case were solved. Second, an analytic model was solved for a plane shear wave incident on a cylindrical hole with an elastic layer. For the expected variation in layer thickness and material properties, the performance of the top crack detection algorithm was not significantly degraded. However, flaw sizing algorithms will be more difficult for the elastic layer case.

A study examining the possible detection of top cracks for holes containing elastic inserts was also presented. A BEM model was applied for the scattering response of an incident shear wave transducer signal by a cylindrical hole with a radial notch, an elastic insert, and a stiffness interface between the hole and the insert. Through comparisons with experimental data, characterization of the interface condition between the hole and the insert was assessed to be a slip bond. A feasible ultrasonic inspection strategy was determined from the simulated and experimental studies. Validation of the approach is presented for both simulated and experimental data. An examination of the sensitivity of the inspection technique to variation in measurement, geometric and material parameters was also presented. Due to model limitations for the corner crack inspection case, the classification algorithm sensitivity for certain inspection parameters is not well understood. Genetic algorithms were used to optimize these parameters using experimental data. Genetic algorithms were shown to be a viable means of optimizing the classification algorithm to indicate valuable features of the inspection problem.

8.2 Recommended Automated Classification Work

The decision to pursue automated classification for an inspection problem depends on the benefit gained versus the cost of implementation. The benefits of implementing automated classification were discussed in Chapter 1. The cost of implementation is based on the required development time, the computational time, and the computational hardware for a particular inspection problem.

One significant issue concerning the application of automated classification for certain inspection problems is the development time and the resulting costs. Considerable time may be required to write, optimize, and validate the classification algorithm, but it only has to be done once for a specific problem. Also, the classification software must interface with the data acquisition hardware to present the results to the operator. It must be checked that, the benefit of automated classification is great enough to justify the time and cost of implementation.

A significant issue concerns the possible lack of robustness and flexibility of automated classification inspection systems. Changes of inspection equipment may reduce the performance of the classification algorithm and thus necessitate retraining. In addition, unexpected variation in material geometry, properties, and condition may produce errors in the automated classification call.

These issues can be partially addressed through straightforward project management strategies. First, during the early stages of the project, the performance benefit of implementing an automated classification procedure must be thoroughly

assessed with respect to the development time and cost. Second, repeated implementation of automated classification builds valuable experience within the project team. Prior experience with in-field variation can aid in both streamlining the training process and focusing validation on the important inspection parameters. Software for classification algorithms, hardware interfaces, and operator interfaces may also be recycled for future projects, thus reducing development time. Third, when feasible, integrating visual inspection 'checks' using the operator interface may be a valuable method for final validation of the classification algorithm during the initial implementation stage while also building confidence with the inspectors.

Several research directions are proposed in order to address these issues. First, improved signal processing techniques should be investigated. Research into multi-dimensional (time and spatial domain) signal processing techniques has been promising and should continue. The spatial signal variation approach presented in Chapter 2 may be used for other inspection problems. Second, incremental learning schemes have been examined for adding adaptability to classification algorithms [86]. Further research is required for the implementation of incremental learning to in-field applications. Third, continued research into selecting the best classification algorithm for an inspection task is needed. Reduction of feature vector complexity was shown to improve the robustness of classification algorithms incorporating neural networks. Genetic algorithms were also presented as a viable approach for efficiently optimizing inspection parameter settings. However, parameter optimization does not directly address the optimal design of the algorithm structure. Since the design process is typically based on the experience of the

engineer, alternative approaches to improve inspection performance may be ignored. Algorithm construction using genetic programming (GP) is proposed as an alternative to solely relying on expert knowledge in determining the structure of a classification algorithm. Genetic programming is a method of evolving a population of programs based on a fitness criteria [87,88]. Individual programs undergo operations similar to genetic algorithms until the program structure meets the desired performance results. Genetic programming can be used to refine an initial algorithm design of the engineer. Genetic programming has been applied to optimizing data mining algorithms for medical databases [88,89]. Research is proposed to determine how genetic programming can be tailored to optimize non-destructive inspection algorithms. Initially, genetic programming might be used to further refine an initial algorithm design.

8.3 Recommended Modeling Work

Additional modeling work is recommended to address a specific issue with the ultrasonic inspection for fatigue cracks about weep holes with a polyurethane coating. A model for the scattering of an incident transducer signal from a cavity with an annular elastic lining and a radial interface crack using a hybrid approach is proposed. The suggested approach incorporates the finite element method (FEM) for the analysis of the region of the crack and the elastic annulus region, and the BEM for the analysis of the external infinite elastic domain. Subsequent parametric studies concerning the crack,

elastic layer, cavity and transducer characteristics are proposed. The focus of the parametric studies should be to understand the effect of the elastic layer on the reflection and transmission of a 'leaky' Rayleigh wave by a radial fatigue crack.

From a general perspective, this work displayed several ways in which modeling benefited algorithm development. Typically, the decision to develop a model for an inspection problem depends on the benefit gained versus the cost of implementation. The benefits of modeling during the development process were discussed in Chapter 1.

Due to several significant issues, the direct use of modeling during the development process has been somewhat limited. Extensive development time is one significant issue. By the time a model can be completed, a rudimentary understanding through experimentation is achieved and thus the model is viewed, often mistakenly, as no longer of great use. Another issue concerns the computational intensive nature of numerical simulations required for non-destructive inspection problems. Typical ultrasonic modeling problems consist of high frequency, broad-band, transient signals and scattering in three dimensions, which often require considerable computational time. Anisotropic and inhomogeneous materials further complicate simulations. These complications often lead engineers to assumptions that reduce solution time but sacrifice model accuracy.

These issues can again be partially addressed through straightforward project management strategies. First, during early stages of the project, the performance benefit of incorporating modeling in the development process must be thoroughly assessed with respect to the development time and cost. Once modeling is determined to be

advantageous, available software packages, either commercial or public domain, should be first explored in order to minimize model development time. Also, experts in academia and industry should be consulted before an extensive modeling program is begun. If model development is required to address a complex inspection problem, a sufficient investment in engineering expertise and computational hardware is required. Finally, if the current level of numerical simulation is unable to represent the inspection problem, empirical modeling remains a final option.

Several research directions are also proposed in order to address these issues. Clearly, more general packages are needed to handle the variety of inspection problems found in industry. Separate packages based on a single solution method such as ray method or finite difference techniques currently exist. Each of these packages can successfully model specific problems, but often fail for other problems due to inherent approximations or excessive computational time. Hybrid models have been proposed to better handle a broader class of modeling problems [90]. In this Dissertation, a hybrid model, incorporating a gaussian beam solution for the incident transducer field, and a BEM solution for the scattered field, was used to solve for the total field response. Further research is necessary to develop modeling techniques that apply the appropriate modeling approach to each portion of the inspection model. Research into expert systems, by which the modeling 'knowledge base' is organized and applied to determine the appropriate modeling approaches for an inspection problem, and genetic programming, to optimally integrate appropriate models would be desirable.

REFERENCES

[1] T.A. Gray, R.B. Thompson, "Use of models to predict ultrasonic NDE reliability", *Review of Progress in QNDE*, v 5, eds. D.O. Thompson & D.E. Chimenti, (Plenum Press, New York, 1986), p. 1986.

[2] J.D. Achenbach, "Measurement models for quantitative ultrasonics", *J. Sound and Vibration*, 159, (1992), p. 385.

[3] L.W. Schmerr Jr., *Fundamentals of Ultrasonic Non-destructive Evaluation*, (Plenum Publ., 1998.)

[4] J.D. Achenbach, "Quantitative non-destructive evaluation", *Inter. Journal of Solids and Structures*, 37, (2000), p. 13.

[5] B.A. Auld, "General electromechanical reciprocity relations applied to the calculation of elastic wave scattering coefficient", *Wave Motion*, 1, (1979), p. 3.

[6] M. Lowe, "Matrix techniques for molding ultrasonic waves in multilayered media", *IEEE Trans Ultrasonic Ferroelectr Freq Control*, v 42, 4, (1995), p. 525-524.

[7] M. Spies, "Simulation of ultrasonic testing of complex-structured materials and components", *Proc IEEE Ultrasonic Symposium*,

[8] A. Lhemery, P. Calmon, I. Lecoeur-Taibi, R. Raillon, L. Paradis, "Modeling tools for ultrasonic inspection of welds", *NDT & E International*, v 33, n 7, (2000), p. 499.

[9] V.K. Kinra, V.R. Iyer, "Ultrasonic measurement of the thickness, phase velocity, density or attenuation of a thin-viscoelastic plate. Part II: the inverse problem", *Ultrasonics*, v 33, 2, (1995), p. 111.

[10] J.L. Rose, J.B. Nestleroth, K. Balasubramaniam, "Elements of a feature-based ultrasonic inspection system", *Material Evaluation*, 42, (1984), p. 210.

[11] L.W. Schmerr, K.E. Christensen, S.M. Nugen, L.S. Koo, C.P. Chiou, "Ultrasonic flaw classification – an expert system approach", Review of Progress in QNDE, v 8, eds. D.O. Thompson & D.E. Chimenti, (Plenum Press, New York, 1989), p. 657.

[12] D. Berry, L. Udpa, S.S. Udpa, "Classification of ultrasonic signals via neural networks", Review of Progress in QNDE, v 10, eds. D.O. Thompson & D.E. Chimenti, (Plenum Press, New York, 1990), p. 697.

[13] S.J. Song, L.W. Schmerr, "Ultrasonic flaw classification in weldments using probabilistic neural networks", *Journal of Nondestructive Evaluation*, v 11, n 2, (1992), p. 69.

[14] K. Zgonc, J.D. Achenbach, Y.C. Lee, "Crack sizing using a neural network classifier trained with data obtained from finite element models", *Review of Progress in QNDE*, v 14, eds. D.O. Thompson & D.E. Chimenti, (Plenum Press, New York, 1995), p. 779.

[15] A.P. Cheng, A. Cheng, R. Rogers, J.D. Achenbach, "A neural network for depth determination of separations between a rubber matrix and reinforcing steel belts", *Review of Progress in QNDE*, v 18, eds. D.O. Thompson & D.E. Chimenti, (Plenum Press, New York, 1999), p. 835.

[16] P.B. Nagy, M. Blodgett, M. Golis, "Weep hole inspection by circumferential creeping waves", *NDT&E International*, 27, n 3, (1994), p. 131.

[17] M. Blodgett, P.B. Nagy, M. Golis, "Weep hole inspection for radial fatigue cracks by circumferential creeping waves", *Review of Progress in QNDE*, Vol. 14, eds. D.O. Thompson & D.E. Chimenti, (Plenum Press, New York, 1995), p. 1963.

[18] W. Hassan, P.B. Nagy, "Circumferential creeping waves around a fluid-filled cylindrical cavity in an elastic media", *J. Acoust. Soc. Am.*, 101, (1997), p. 2496.

[19] W. Hassan, P.B. Nagy, "Feasibility of fatigue crack detection in fluid-filled cylindrical holes using circumferential creeping waves", *Review of Progress in QNDE*, Vol. 16, eds. D.O. Thompson & D.E. Chimenti, (Plenum Press, New York, 1997), p. 43.

[20] W. Hassan, P.B. Nagy, "On the anomalously low attenuation of the leaky Rayleigh wave in a fluid-filled cylindrical cavity", *J. Acoust. Soc. Am.*, 104, (1998), p. 1246.

[21] W. Hassan, P.B. Nagy, "Doubly-leaky Rayleigh wave propagation around a fluid-filled cylindrical cavity", *Review of Progress in QNDE*, Vol. 18, eds. D.O. Thompson & D.E. Chimenti, (Plenum Press, New York, 1999), p. 167.

[22] J.C. Aldrin, J.D. Achenbach, G.A. Andrew, C. P'an, B. Grills, R.T. Mullis, F.W. Spencer, M. Golis, "Case study for the implementation of an automated ultrasonic technique to detect fatigue cracks in aircraft weep holes", *Materials Evaluation*, (to be published.)

[23] J.C. Aldrin, A. Cheng, J.D. Achenbach, G.A. Andrew, R.T. Mullis, "Detection of fatigue cracks in weep holes using neural networks", *Review of Progress in QNDE*, (AIP, 2000), p. 1979.

[24] J.D. Achenbach, A.K. Gautesen, H. McMaken, *Ray Methods for Waves in Elastic Solids*, (Pitman Publ., Boston , 1982.)

[25] Y. Niwa, S. Hirose, M. Kitahara, "Application of the boundary integral equation (BIE) method to transient response analysis of inclusion in a half space", *Wave Motion*, 8, (1986), p. 77.

[26] G.D. Manolis, D.E. Beskos, *Boundary Element Methods in Elastodynamics*, (Unwin Hyman, Chapman & Hall, London, 1988.)

[27] A.A. Becker, *Boundary Element Method in Engineering* (London, McGraw-Hill, 1992.)

[28] J. Dominguez, *Boundary Elements in Dynamics* (Computational Mechanics Publications, Southampton, Boston, 1993.)

[29] J.L. Rose, J.B. Nestleroth, K. Balasubramaniam, "Utility of feature mapping in ultrasonic non-destructive evaluation", *Ultrasonics*, 26, (1988), p. 124.

[30] V. Schmitz, S. Chakhlov, W. Müller, "Experiences with synthetic aperture focusing technique in the field", *Ultrasonics*, 38, (2000), p. 731.

[31] L. Tao, X. R. Ma, H. Tian, Z. X. Guo, *J Sound Vib*, 193, (1996), p. 1015.

[32] Q. Tian, X. Li, N.M. Bilgutay, "Multiple target detection using split spectrum processing and group delay moving entropy", *IEEE Trans Ultrason Ferroelec Freq Cntrl*, Vol. 42, 6, (1995), p. 1076.

[33] P. M. Gammell, *Ultrasonics*, Vol. 19, (1981), p. 73.

[34] D.E. Newland, *An Introduction to Random Vibrations, Spectral and Wavelet Analysis*, (Longman, Essex, 1993.)

[35] S. Moubarik, D. De Vadder, P. Benoist, *Review of Progress in QNDE*, Vol. 12, (1993), p. 727.

[36] M. Wax, T. Kailath, "Detection of signals by information theoretic criteria", *IEEE Trans Signal Processing*, Vol. 33, 2, (1985), p. 387.

[37] B. G. Lindsay, P. Basak, "Multivariate normal mixtures: a fast consistent method of moments", *Journal of the American Statistical Association*, Vol. 88, 442, (1993) p. 468.

[38] A.K. Kromine, P.A. Fomitchov, S. Krishnaswamy, J.D. Achenbach, *Materials Evaluation*, Vol. 58, n 2, (2000), p. 173.

[39] G. Corneloup, J. Moysan, D. Francois, *Review of Progress in QNDE*, Vol. 15, (1996), p. 917.

[40] J. Kim, P. Ramuhalli, L. Upda, S. Upda, "Multidimensional signal processing for ultrasonic signal classification" *Review of Progress in QNDE*, (AIP, to be published in 2001.)

[41] U.S. Department of Defense, MIL-HDBK-1823 Nondestructive Evaluation System Reliability Assessment, 30 April 1999.

[42] D.A. Mendelson, J.D. Achenbach, L.M. Keer, "Scattering of elastic waves by a surface breaking crack", *Wave Motion*, 2, (1980), p. 277.

[43] Y. C. Angel, J. D. Achenbach, "Reflection and transmission of obliquely incident Rayleigh waves by a surface-breaking crack", *J. Acoust Soc Am*, 75, (1984), p 313.

[44] C.L. Scandrett, J. D. Achenbach, "Time-domain finite difference calculations for interaction of an ultrasonic wave with a surface-breaking crack", *Wave Motion*, 9, (1987), p. 171.

[45] C. Zhang, J. D. Achenbach, "Scattering of body waves by an inclined surface-breaking crack", *Ultrasonics*, Vol. 26, 3, (1988), p. 132.

[46] Z.L. Li, J. D. Achenbach, "Reflection and transmission of Rayleigh surface waves by a material interphase", *J Appl Mech*, 58, (1991), p. 688.

[47] B. Rulf, "Rayleigh waves on curved surfaces", *J Acoust Soc Am*, Vol. 45, 2, (1969), p. 493.

[48] D. Burdreck, "Ultrasonic scattering from a crack which emanates from a rivet hole", *Review of Progress in QNDE*, Vol. 12, (1993), p. 83.

[49] C.C. Mow, L.J. Mente, "Dynamic stresses and displacements around cylindrical discontinuities due to plane harmonic shear waves", *J. Appl. Mech.*, Vol. 30, (1963), p. 598.

[50] S.G. Solomon, H. Uberall, K.B. Yoo, "Mode conversion and resonance scattering of elastic waves from a cylindrical fluid-filled cavity", *Acustica*, Vol. 55, (1984), p. 147.

[51] C.C. Mow, J.W. Workman, "Dynamic stresses around a fluid-filled cavity", *J. Appl. Mech*., Vol. 33, (1966), p. 793.

[52] Y.H. Pao, C.C. Mow, *Diffraction of Elastic Waves and Dynamics Stress Concentrations*, (Crane, Russak & Company Inc., New York, 1971.)

[53] Conversation with Floyd W. Spencer of Sandia National Laboratory, (2000.)

[54] K.V. Mardia, "Test of univariate and multivariate normality", *Handbook of Statistics*, Vol. 1, (North-Holland, New York, 1980), pp. 279-320.

[55] G. Box and G. Tiao, *Bayesian Inference in Statistical Analysis*, (John Wiley and Sons, Inc., New York, 1992.)

[56] I.A. Viktorov, "Rayleigh-type waves on a cylindrical surface", *Soviet Phys. – Acoust., 45*, (1958), p. 131.

[57] I.A. Viktorov, *Rayleigh and Lamb Waves*, (Plenum Press, New York, 1967.)

[58] J. Qu, Y. Berthelot, Z. Li, "Dispersion of guided circumferential waves in a circular annulus", *Review of Progress in Quantitative NDE*, Vol. 15, (1996), p. 169.

[59] G. Liu, J. Qu, "Guided circumferential waves in a circular annulus", *Trans ASME*, 65, (1998), p. 424.

[60] R. Stoneley, "Elastic waves at the surface of separation of two solids", *Proceedings of the Royal Society* (London), 106, (1924), p. 416.

[61] J.D. Achenbach and H.I. Epstein, "Dynamics interaction of a layer and a half space", *Journal of the Engineering Mechanics*, American Society of Civil Engineers, Vol. 93, EM 5, (1967), p. 27.

[62] H.I. Epstein, "The Effect of curvature on stoneley waves", *J. Sound Vibration*, 46, (1976), p. 59.

[63] H.I. Epstein, "Circumferential waves in a composite circular cylinder", *J. Sound Vibration*, 48, (1976), p. 57.

[64] C. Valle., J. Qu., L.J. Jacobs, "Guided circumferential waves in layered cylinders", *International Journal of Engineering Science*, 37, (1999), p. 1369.

[65] U. Kawald, C. Desmet, W. Lauriks, C. Glorieux, J. Thoen, "Investigation of the dispersion relations of surface acoustic waves propagating on a layered cylinder", *J. Acoust. Soc. Am.*, 99, (1996), p. 926.

[66] C. Valle., C, J. Qu., L. J. Jacobs, "On the dispersion and displacement distribution of circumferential waves in a composite circular cylinder", *Review of Progress in QNDE*, Vol. 18, eds. D.O. Thompson & D.E. Chimenti, (Plenum Press, New York, 1999), p. 247.

[67] A.N. Sinclair, R.C. Addison Jr., "Acoustic diffraction spectrum of a SiC fiber in a solid elastic medium", *J. Acoust. Soc. Am.*, 94, (1993), p. 1126.

[68] S.I. Rokhlin, W. Huang, Y.C. Chu, "Ultrasonic scattering and velocity methods for characterization of fibre-matrix interphases", *Ultrasonics*, Vol. 33, 5, (1995), p. 351.

[69] I. J. Thompson, A R. Barnett, "Coulomb and Bessel functions of complex argument and order", *Journal of Computational Physics*, 64, (1986), p. 490.

[70] V. Sastry, "Algorithms for the computation of Hankel functions of complex order", *Numerical Algorithms*, 5, (1993), p. 621.

[71] B. Davies, "Locating the zeros of an analytic function", *Journal of Computational Physics*, 66, (1986), p. 36.

[72] K. Atkinson, *An Introduction to Numerical Analysis*, (John Wiley & Sons, New York, 1989.)

[73] B. Hartman, "Acoustic properties", *Physical Properties of Polymers Handbook*, Editor. J. E. Mark, (AIP Press, Woodbury, New York, 1996), p. 677.

[74] R.M. White, "Elastic wave scattering at a cylindrical discontinuity in a solid", *J. Acoust. Soc. Am.*, 30, (1958), p. 771.

[75] P. Beattie, R.C. Chivers, L.W. Anson, "Ultrasonic backscattering from solid cylindrical inclusions in solid elastic matrices: A comparison of theory and experiment", *J. Acoust. Soc. Am.*, 94, (1993), p. 3421.

[76] P.B. Nagy, "Ultrasonic classification of imperfect interfaces", *Journal of Nondestructive Evaluation*, Vol. 11, (1992), p. 127.

[77] W. Huang, S.I. Rokhlin, "Spring and asymptotic boundary condition models for study of scattering by thin cylindrical interphases", *Review of Progress in QNDE*, Vol. 15, eds. D.O. Thompson & D.E. Chimenti, (Plenum Press, New York, 1996), p. 121.

[78] D.E. Goldberg, *Genetic Algorithms in Search, Optimization and Machine Learning*, (Addison-Wesley Publishing Co., Inc., Cambridge, MA, 1989.)

[79] M. Mitchell, *An Introduction to Genetic Algorithms*, (MIT Press, Cambridge, MA, 1996.)

[80] F. Thollon, N. Burais, "Geometric optimization of sensors for eddy current Non Destructive Testing and Evaluation", *IEEE Trans on Magnetics*, (1995), Vol. 31, 3, p. 2026.

[81] T. Heckman, J. Krumm, "Searching for contours", *Proc SPIE Int Soc Opt Eng*, 2666, (1996), p. 223.

[82] T. Sawaragi, J. Umemura, O. Katai, S. Iwai, "Fusing multiple data and knowledge sources for signal understanding by genetic algorithm", *IEEE Trans Ind Electron*, (1996), Vol. 43, 3, p. 411.

[83] K. Balasubramaniam, "Experimental determination of material stiffness constants for advanced composites using Genetic Algorithms", *Proc SPIE Int Soc Opt Eng* , 2921, (1997), p. 116.

[84] T. Olofsson, T. Stepinski, "Maximum a posteriori deconvolution of sparse ultrasonic signals using genetic optimization", *Ultrasonics*, 37, (1999), p. 423.

[85] Web page of M.B. Gordy, http://mgordy.tripod.com.

[86] R. Polikar, L. Upda, S. Upda, "Incremental learning of ultrasonic weld inspection signals" *Review of Progress in QNDE*, (AIP, to be published in 2001.)

[87] J.R. Koza, Genetic Programming: On the Programming of Computers by Means of Natural Selection, (Bradford/MIT Press, Cambridge, MA, 1992.)

[88] C.C. Bojarczuk, H.S. Lopes, A.A. Freitas, "Genetic programming for knowledge discovery in chest-pain diagnosis", *IEEE Eng Med Biol*, (2000), Vol. 19, 4, p. 38.

[89] M.L. Wong, W. Lam, K.S. Leung, P.S. Ngan, J.C.Y. Cheng, "Discovering knowledge from medical databases using evolutionary algorithms", *IEEE Eng Med Biol*, (2000), Vol. 19, 4, p. 45.

[90] I.T. Lu, H.K. Jung, "A hybrid (boundary elements)-(finite elemnts)-ray-mode method for wave scattering by inhomogeneous scatterers in a waveguide", *J. Acoust. Soc. Am*., 87, (1990), p. 988.

[91] D.E. Beskos, "Boundary element methods in dynamic analysis", *Appl Mech Rev*, Vol. 40, 1, (1987), p. 1.

[92] A. Lhemery, "An analytic expression for the transient ultrasonic field radiated by a shear wave transducer in solids", *J. Acoust. Soc. Am*., 96, (1994), p. 3787.

[93] J.C. Aldrin, J.D. Achenbach, "Refined detection of cracks in weep holes using spatial signal variation" *Review of Progress in QNDE*, (AIP, to be published in 2001.)

[94] *Metals Handbook (10th ed.) – Vol. 2 Properties and Selection: Nonferrous Alloys & Special Purpose Materials*, (ASTM Int, 1999.)

APPENDIX

APPENDIX A – PARAMETER SETTINGS FOR BEM SIMULATIONS

A.1 General Features of BEM Simulation

In order to minimize the computational time for the solution of these high frequency elastic wave scattering problems, the following model was chosen:

BEM Simulation Approach

- 2D Frequency domain boundary element method
- Use Fourier transforms to convert transient problem into series of frequency domain problems
- Typically, the crack case would be modeled using two separate domains. However, discritization of our problem in two domains leads to much larger systems of equations to solve. To obtain a good solution with much less computational time, a single boundary incorporating a cylindrical hole with a open notch (of finite width) was used. This definition results in a single domain.
- A notch width of 0.010" was determine to be a good value to use for the simulations in order to minimize the error due to boundary points being location in close proximity to one another.
- Quarter node elements were used to approximate the singularity at the tip.
- Calculation of the transducer response is performed by approximating the location of the transducers in the elastic media, calculating a series of points along a line of the transducer, and combining these points into a signal voltage response (assuming a Gaussian distribution across the transducer).

Total Field Solution Steps

- Define Transient Incident Field in Time Domain
- Calculate Tractions from Incident Field at Hole Boundary
- Apply Counter Traction to Boundary to Solve for Scattered Field Problem
- Convert Transient Stress Conditions from Time to Frequency Domain via FFT
- Solve Series of Frequency Domain BEM problems (Dominguez et al)
- Convert Resulting Scattered Field Response to Time Domain Solution via Inverse FFT
- Scattered and Free Field Responses Summed to Obtain Total Transient Response

See reference for specific details of boundary element simulation [25-28,91].
Tables A.1-7 shows typical parameter setting for the BEM simulations performed.
Figure A.1 displays the used interface used to perform these BEM simulation.

Table A.1. Typical input parameters.

Number of Time Steps	512 – empty hole case (1048 – elastic insert hole case) (2048 – fluid-filled hole case)
Transducer Center Frequency	3.71 MHz – measured for old transducer (5.00 MHz – measured for new transducer)
Samples per Period	6
Transient Input	Gaussian Beam – transient pulse defined by sinusoid with Gaussian distribution * (Lhemery shear transducer model [92])
κ (for transient Gaussian pulse)	10 – wide pulse (2.5 – tight pulse)
Start Frequency Analysis Step	44 – empty hole case (90 – elastic insert hole case) (180 – fluid-filled hole case)
End Frequency Analysis Step	127 – empty hole case (250 – elastic insert hole case) (500 – fluid-filled hole case)

* See Figure 4.5. Transient pulse (a) in time domain, and (b) frequency spectrum.

Table A.2. Typical transducer parameters.

Incident Elastic Wave Type	Shear
Width of Transducers	0.250 in.
Transmitting Transducer Location in Y dir.	-0.862 in – pulse-echo for weep hole
Transmitting Transducer Location in X dir.	-0.141 in – pulse-echo for weep hole (corresponds to 0.200 in from reference on wing surface)
Space in Y dir. Between Transmitting and Receiving Transducers	0.0483 in.

Table A.3. Typical elastic media parameters.

Material	*Aluminum*
Real Shear Modulus	26.45 GN/m^2
Density	2700 kg/m^3
Poisson's Ratio	0.33
Damping	0.0005
2D Model Type	Plane Stress (for thin plates)

Table A.4. Typical cavity parameters.

Material	*Aluminum*
Radius of Cavity	0.125 in. – typical weep hole (0.09375 in. – typical rib clip hole)
Number of Elements	100 – typical weep hole (76 – typical rib clip hole)

Table A.5. Typical fluid fill cavity parameters.

Material	*Water*
Real Shear Modulus	2.189 GN/m^2
Density	999 kg/m^3
Damping	0.0005

Table A.6. Typical notch parameters.

Typical Length	0.070 in.
Width	0.010 in.
Angular Location of Crack	45
Number of Elements	18
Notch Tip Condition	Flat Notch End (Point at tip – with singularity) (Point at tip – no singularity)
Taper Condition	Parallel Sides (Taper to point) (Taper to point)
Elements at Notch End	2

Table A.7. Typical results parameters.

Solution Points per Transducer	20
Grid boundaries ranges in X direction	-1 to 3, in radii
Solution Points per Transducer	25 points/radii
Grid boundaries ranges in X direction	-2,2, in radii
Solution Points per Transducer	25 points/radii

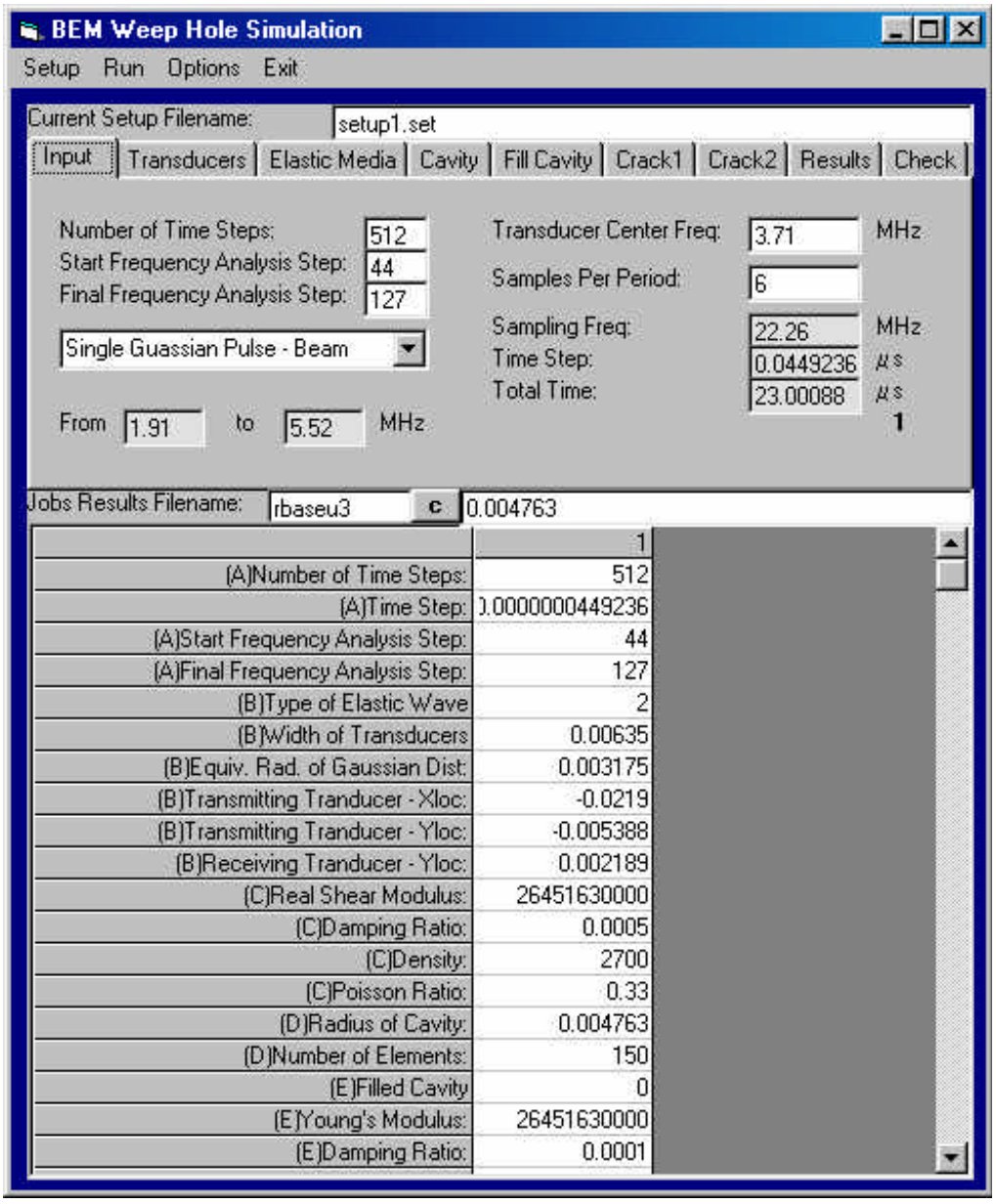

Figure A.1. BEM weep hole simulation user interface.

A.2 BEM Simulation of Bottom Notch About Weep Hole (Section 2.2)

The details of this simulation have been previously presented [93].

Table A.8. Bottom notch inspection simulation parameters.

Incident Elastic Wave Type	Shear
Width of Transducers	0.250 in.
Transmitting Transducer Location in Y dir.	-0.640 in – pulse-echo for weep hole
Transmitting Transducer Location in X dir.	0.085 in – pulse-echo for weep hole (corresponds to +0.120 in from reference on wing surface)
Space in Y dir. Between Transmitting and Receiving Transducers	0.0483 in.
Lengths	0.070 (and 0.018) in.
Width	0.010 in.
Angular Location of Crack	-135 (and -145) in.
Number of Elements	18 (and 8)

A.3 BEM Simulation of Top Notch about Weep Hole (Sections 3.2, 4.4, 4.5, 4.6)

The details of this simulation have been previously presented [23] and are listed in Tables A.1-7.

A.4 BEM Simulation of Top Notch about Fluid-Filled Weep Hole (Sections 5.3, 5.4)

Table A.9. Specific parameters for fluid-fill case.

Number of Time Steps	2048 – fluid-filled hole case
Start Frequency Analysis Step	180 – fluid-filled hole case
End Frequency Analysis Step	500 – fluid-filled hole case
Material	*Water*
Real Shear Modulus	*2.189 GN/m^2*
Density	*999 kg/m^3*
Damping	*0.0005*
Notch Length	0.070 in.
Notch Width	0.010 in.
Angular Location of Crack	45
Number of Elements	18
Notch Tip Condition	Flat Notch End
Taper Condition	Parallel Sides
Fluid in Notch	YES
Elements at Notch End	2

A.5 BEM Simulation of Top Notch about Cylindrical Hole Containing an Elastic Insert, Top Notch and Stiffness Interface (Sections 7.4, 7.6)

Table A.10. Specific parameters for elastic insert case.

Number of Time Steps	1024 – elastic insert hole case
Transducer Center Frequency	5.00 MHz – measured for new transducer
Start Frequency Analysis Step	90 – elastic insert hole case
End Frequency Analysis Step	250 – elastic insert hole case
Transmitting Transducer Location in Y dir.	-0.807 in – pulse-echo for weep hole
Transmitting Transducer Location in X dir.	-0.085 in – pulse-echo for weep hole (corresponds to -0.120 in from reference on wing surface)
Radius of Cavity	0.09375 in. – typical rib clip hole
Number of Elements	76 – typical rib clip hole
Infinite elastic medium	7075-T6 Aluminum [94]
- Real Shear Modulus	- 26.9 GN/m^2
– Density	- 2800 kg/m^3
- Poisson's Ratio	- 0.33
- Damping	- 0.0005
- 2D Model Type	- Plane Stress (for thin plates)
Insert Material	7050-T73 Aluminum [94] (and Steel)
- Real Shear Modulus	- 26.9 GN/m^2 - (83.0 GN/m^2)
– Density	- 2830 kg/m^3 - (7700 kg/m^3)
- Poisson's Ratio	- 0.33 - (0.28)
- Damping	- 0.0005 - (0.0005)
Notch Length	0.070 in.
Notch Width	0.010 in.
Angular Location of Crack	45
Number of Elements	18
Notch Tip Condition	Flat Notch End
Taper Condition	Parallel Sides
Fluid in Notch	Empty Notch
Elements at Notch End	2
Normal interface stiffness	$K_N = 1e17$
Tangential interface stiffness	$K_T = 1e11$

APPENDIX B – DISPERSION RELATION

$$[\mathbf{M}]=\begin{Bmatrix}
\begin{bmatrix}\left(2+\frac{2}{n}-\frac{b_1^{\,2}}{g^2}\right)JA_{1a0}\\ -\frac{2a_1}{gn}JA_{1a}\end{bmatrix} & \begin{bmatrix}\left(2+\frac{2}{n}-\frac{b_1^{\,2}}{g^2}\right)YA_{1a0}\\ -\frac{2a_1}{gn}YA_{1a}\end{bmatrix} & 2\begin{bmatrix}\frac{b_1}{g}JB_{1a}\\ -\left(1+\frac{1}{n}\right)JB_{1a0}\end{bmatrix} & 2\begin{bmatrix}\frac{b_1}{g}YB_{1a}\\ -\left(1+\frac{1}{n}\right)YB_{1a0}\end{bmatrix} & 0 & 0\\
2\begin{bmatrix}\frac{a_1}{g}JA_{1a}\\ -\left(1+\frac{1}{n}\right)JA_{1a0}\end{bmatrix} & 2\begin{bmatrix}\frac{a_1}{g}YA_{1a}\\ -\left(1+\frac{1}{n}\right)YA_{1a0}\end{bmatrix} & \begin{bmatrix}\left(2+\frac{2}{n}-\frac{b_1^{\,2}}{g^2}\right)JB_{1a0}\\ -\frac{2b_1}{gn}JB_{1a}\end{bmatrix} & \begin{bmatrix}\left(2+\frac{2}{n}-\frac{b_1^{\,2}}{g^2}\right)YB_{1a0}\\ -\frac{2b_1}{gn}YB_{1a}\end{bmatrix} & 0 & 0\\
g\begin{bmatrix}2-b_1^{\,2}\\ -\frac{2}{n}(a_1JA_1-1)\end{bmatrix} & g\begin{bmatrix}2-b_1^{\,2}\\ -\frac{2}{n}(a_1YA_1-1)\end{bmatrix} & 2g\begin{bmatrix}b_1JB_1\\ -1-\frac{1}{n}\end{bmatrix} & 2g\begin{bmatrix}b_1YB_1\\ -1-\frac{1}{n}\end{bmatrix} & \begin{bmatrix}2-b^2\\ -\frac{2}{n}(aHA^{(1)}-1)\end{bmatrix} & 2\begin{bmatrix}bHB^{(1)}\\ -1-\frac{1}{n}\end{bmatrix}\\
2g\begin{bmatrix}a_1JA_1\\ -1-\frac{1}{n}\end{bmatrix} & 2g\begin{bmatrix}a_1YA_1\\ -1-\frac{1}{n}\end{bmatrix} & g\begin{bmatrix}2-b_1^{\,2}\\ -\frac{2}{n}(b_1JB_1-1)\end{bmatrix} & g\begin{bmatrix}2-b_1^{\,2}\\ -\frac{2}{n}(b_1YB_1-1)\end{bmatrix} & -2\begin{bmatrix}1+\frac{1}{n}\\ -aHA^{(1)}\end{bmatrix} & -\begin{bmatrix}b^2-2+\\ \frac{2}{n}(bHB^{(1)}-1)\end{bmatrix}\\
a_1JA_1-1 & a_1YA_1-1 & 1 & 1 & aHA^{(1)}-1 & 1\\
1 & 1 & b_1JB_1-1 & b_1YB_1-1 & 1 & bHB^{(1)}-1
\end{Bmatrix}$$

where: $k=\frac{\omega}{c},\alpha=\frac{c}{c_L},\beta=\frac{c}{c_T},\alpha_1=\frac{c}{c_{1,L}},\beta_1=\frac{c}{c_{1,T}},\gamma=\frac{\rho_1}{\rho},\delta=\frac{\rho_1}{\rho},g=\frac{b}{a},h=b-a$, $HA^{(1)}=\frac{H_{n-1}^{(1)}(\alpha kb)}{H_n^{(1)}(\alpha kb)}$, $HB^{(1)}=\frac{H_{n-1}^{(1)}(\beta kb)}{H_n^{(1)}(\beta kb)}$,

$$JA_1 = \frac{J_{n-1}(\boldsymbol{a}_1 kb)}{J_n(\boldsymbol{a}_1 kb)},\ JB_1 = \frac{J_{n-1}(\boldsymbol{b}_1 kb)}{J_n(\boldsymbol{b}_1 kb)}, JA_{1a} = \frac{J_{n-1}(\boldsymbol{a}_1 ka)}{J_n(\boldsymbol{a}_1 kb)},\ JB_{1a}^{(1)} = \frac{J_{n-1}(\boldsymbol{b}_1 ka)}{J_n(\boldsymbol{b}_1 kb)}, JA_{1a0} = \frac{J_n(\boldsymbol{a}_1 ka)}{J_n(\boldsymbol{a}_1 kb)}, JB_{1a0}^{(1)} = \frac{J_n(\boldsymbol{b}_1 ka)}{J_n(\boldsymbol{b}_1 kb)},$$

$$YA_1 = \frac{Y_{n-1}(\boldsymbol{a}_1 kb)}{Y_n(\boldsymbol{a}_1 kb)},\ YB_1 = \frac{Y_{n-1}(\boldsymbol{b}_1 kb)}{Y_n(\boldsymbol{b}_1 kb)}, YA_{1a} = \frac{Y_{n-1}(\boldsymbol{a}_1 ka)}{Y_n(\boldsymbol{a}_1 kb)},\ YB_{1a}^{(1)} = \frac{Y_{n-1}(\boldsymbol{b}_1 ka)}{Y_n(\boldsymbol{b}_1 kb)},\ YA_{1a0} = \frac{Y_n(\boldsymbol{a}_1 ka)}{Y_n(\boldsymbol{a}_1 kb)},\ YB_{1a0}^{(1)} = \frac{Y_n(\boldsymbol{b}_1 ka)}{Y_n(\boldsymbol{b}_1 kb)}.$$

APPENDIX C – OPTIMIZATION PROBLEMS USING GENETIC ALGORITHMS

The genetic algorithm optimization routine used for the optimization problem was adapted from a program written by Michael Gordy [89]. Table C.1 displays the parameter settings used for the genetic algorithm during the optimization process.

Table C.1. Genetic algorithm optimization parameter settings.

Parameter	**Value**
size of generation	10
crossover rate (between 0 and 1)	0.5
mutation rate (between 0 and 1)	0.5
number of iterations best is reinserted into generation	5
solution precision	1e-4

Table C.2 displays the constraints for the 11 optimization parameters. The measurement approach is similar to prior top crack detection algorithms. For the grid of spatial location for the pulse-echo (CPE) and pitch-catch (CPC) data, the peak-to-peak measure within the time gate is calculated for each spatial location, and an average over the spatial grid is calculated.

The time variables, X(1), X(2), X(3), and X(4), are integers with units of 0.01·μsec. The units for variable X(5) are 0.01·μsec per spatial increment. Variables X(6), X(7), X(8), X(9), X(10), and X(11), are in terms of incremental transducer spatial steps. All spatial increments are 0.020''. The spatial location variables in the X direction, X(6) and X(8), begin one spatial increment from the specular reference location.

Since the inspection is performed at discrete times and spatial locations, all 11 optimization parameters were represented by discrete variables. The incremental range for each inspection variable is also given in Table C.2. A binary encoding of the parameters was used to simplify the implementation of genetic algorithms as the optimization routine. Table C.3 displays the binary encoding for each parameter constraint. The equation,

$$X(n) = F_{add}(n) + F_{mult}(n) \cdot Y(n), \tag{C.1}$$

represents the relation between the binary encoding and the actual parameter value. Table C.4 lists the changes to the optimization parameters for two variables when considering optimization of left and right 'corner' notch locations.

Table C.2. Search parameter constraints.

X(n)	Parameter	X_{low}	X_{high}	N	F_{add}	F_{mult}
X(1)	Time gate start CPC	100	400	16	100	20
X(2)	Time gate width CPC	25	200	8	25	25
X(3)	Time gate start CPE	160	460	16	160	20
X(4)	Time gate width CPE	25	200	8	25	25
X(5)	Time/spatial adjust for every 0.020" step	18	25	8	18	1
X(6)	Spatial X gate start CPC	1	16	16	1	1
X(7)	Spatial X gate width CPC	1	8	8	1	1
X(8)	Spatial X gate start CPE	1	16	16	1	1
X(9)	Spatial X gate width CPE	1	8	8	1	1
X(10)	Spatial Y gate start - both	1	4	4	1	1
X(11)	Spatial Y gate end - both	7	10	4	1	1

Table C.3. Binary encoded parameter constraints.

Y(n)	Parameter	Y_{low}	Y_{high}	bits
Y(1)	Time gate start CPC	*0*	15	4
Y(2)	Time gate width CPC	*0*	7	3
Y(3)	Time gate start CPE	*0*	15	4
Y(4)	Time gate width CPE	*0*	7	3
Y(5)	Time/spatial adjust for every 0.020" step	*0*	7	3
Y(6)	Spatial X gate start CPC	*0*	15	4
Y(7)	Spatial X gate width CPC	*0*	7	3
Y(8)	Spatial X gate start CPE	*0*	15	4
Y(9)	Spatial X gate width CPE	*0*	7	3
Y(10)	Spatial Y gate start - both	*0*	3	2
Y(11)	Spatial Y gate end - both	*0*	3	2

- Total number of bits for individual population member is 35.
- Total possible parameter setting combinations is $2^{35} = 3.43 \times 10^{10}$.

Table C.4. Specific parameter constraints for right and left 'corner' notch classification.

Corner Notch	X(n)	Parameter	X_{low}	X_{high}	N	F_{add}	F_{mult}
Left	X(10)	Spatial Y gate **start** – both	1	4	4	1	1
Left	X(11)	Spatial Y gate **width** - both	1	4	4	1	1
Right	X(10)	Spatial Y gate **end** – both	7	10	4	7	1
Right	X(11)	Spatial Y gate **width** - both	1	4	4	1	1